Original Article

Prognostic and immunological significance of peroxisome proliferator-activated receptor gamma in hepatocellular carcinoma based on multiple databases

Chaoban Wang, Shiwen Yu, Rengcheng Qian, Shaohe Chen, Chengjun Dai, Xiaoou Shan

Department of Pediatric Endocrine, Wenzhou Yuying Children's Hospital, The Second Affiliated Hospital to Wenzhou Medical University, Wenzhou, China

Contributions: (I) Conception and design: C Wang, X Shan; (II) Administrative support: X Shan; (III) Provision of study materials or patients: None; (IV) Collection and assembly of data: C Wang, R Qian, C Dai, S Yu, S Chen; (V) Data analysis and interpretation: C Wang, R Qian, C Dai, S Yu, S Chen; (VI) Manuscript writing: All authors; (VII) Final approval of manuscript: All authors.

Correspondence to: Prof. Xiaoou Shan. Department of Pediatric Endocrine, Wenzhou Yuying Children's hospital, The Second Affiliated Hospital, Wenzhou Medical University, Wenzhou, China. Email: sssxooo@sina.com.

Background: Peroxisome proliferator-activated receptor gamma (PPARG) plays some roles in preventing liver disease progression to hepatocellular carcinoma. However, there is limited information about the function of PPARG of in hepatocellular carcinoma. This study aimed to determine the significance of PPARG in immunological response and as a biomarker for hepatocellular carcinoma survival.

Methods: We investigated the expression, prognosis, Kyoto Encyclopedia of Genes and Genomes/Gene Ontology biological process enrichment, and immune significance of PPARG using data from three databases—The Cancer Genome Atlas, International Cancer Genome Consortium, and Gene Expression Omnibus—through bioinformatics analysis as well as experimental verification in proliferation function of PPARG in HepG2 cell.

Results: High PPARG expression in hepatocellular carcinoma tissues positively correlated with *TP53* mutation, and predicted poor prognosis. The results of enrichment and immune infiltration showed that PPARG negatively correlated with the complement system and macrophage infiltration, and laboratory results support that PPARG regulate proliferation of HepG2 cell.

Conclusions: PPARG is upregulated in hepatocellular carcinoma and it correlates with a worse prognosis. Moreover, PPARG may play an important role in the cell proliferation, complement system and immune cell infiltration in hepatocellular carcinoma.

Keywords: Hepatocellular carcinoma (HCC); peroxisome proliferator-activated receptor gamma (PPARG); prognosis; complement

Submitted Jan 06, 2022. Accepted for publication Apr 12, 2022.
doi: 10.21037/tcr-21-2853
View this article at: https://dx.doi.org/10.21037/tcr-21-2853

Introduction

Primary liver cancer is the third leading cause of cancer-related deaths, with 905,677 new cases reported worldwide in 2020 (1). Hepatocellular carcinoma (HCC) represents 75–85% of primary liver cancers, and has several risk factors, including hepatitis B virus (HBV), hepatitis C virus, alcohol, metabolic syndrome, diabetes, obesity, and nonalcoholic fatty liver disease (NAFLD) (2). Patients with HCC have a poor survival rate. In the United States, the 2-year survival rate for HCC is <50%, and the 5-year survival rate is only 10% (1). The conventional models, such as tumor, nodes, metastasis (TNM) staging, vascular invasion, and other parameters, help predict HCC prognosis; however, considering the heterogeneity of HCC,

the predictive efficacy remains far from satisfactory (3). Thus, the identification of reliable biomarkers as predictors or potential therapeutic targets is urgently needed.

Peroxisome proliferator-activated receptor gamma (PPARG) is a nuclear receptor that binds to peroxisome proliferator response elements (PPREs) and regulates transcription of target genes involved in energy metabolism, cellular development, and differentiation (2). The anti-inflammatory effects of PPARG have subsequently been elucidated. Several studies have shown that upregulation of PPARG plays an anti-inflammatory role and prevents the occurrence of liver cancer (3). Additionally, a previous study by our group found PPARG to negatively correlate with the inflammatory response in NAFLD (4). PPARG agonism indirectly inhibits hepatic macrophage infiltration and reduces steatosis, inflammation, and fibrosis in NAFLD mouse models (5). Moreover, simvastatin (a cholesterol-lowering drug) inhibits tumor growth by suppressing the hypox inducible factor 1-α/PPARG/Pyruvate Kinase M2 axis, which indicates a relationship between PPARG and cell proliferation in HCC (6).

Briefly, many studies demonstrated that PPARG plays a role in preventing liver cancer; however, the role of PPARG in HCC remains unknown. Before further studying the role of PPARG in HCC, it is necessary to understand the possible prognostic effects of PPARG in HCC patients and the underlying mechanisms, which may help us promote the development of drugs targeting PPARG. Bioinformatics is a great tool to comprehensively analyze clinical data to determine the prognostic impact of PPARG and identify multiple potential mechanisms associated with PPARG through analysis of expression profile data. In this study, we investigated the expression, prognosis, Kyoto Encyclopedia of Genes and Genomes/Gene Ontology (KEGG/GO) biological process enrichment, and immune significance of PPARG by bioinformatics analyses of data from three databases—the Cancer Genome Atlas (TCGA), International Cancer Genome Consortium (ICGC), and Gene Expression Omnibus (GEO). We present the following article in accordance with the MDAR reporting checklist (available at https://tcr.amegroups.com/article/view/10.21037/tcr-21-2853/rc).

Methods

Data sources and description

A single database may cause bias; therefore, we used four databases (ONCOMINE, TCGA, ICGC, and GEO databases) for PPARG expression differential analysis and three sources [TCGA-liver hepatocellular carcinoma (LIHC), ICGC-LIRI, and GEO-GSE14520] for comprehensive analysis, which included expression and clinical data. The study was conducted in accordance with the Declaration of Helsinki (as revised in 2013). ONCOMINE database: ONCOMINE database (www.oncomine.org) is an online cancer microarray database including RNA sequencing (RNA-Seq) data. In this study, PPARG mRNA expression and the P value between cancer tissues and adjacent normal control samples were obtained from the ONCOMINE database. The cut-off values of the P value and fold change were set as 0.05 and 1.5, respectively. The mRNA data type was used, and the gene rank was specified as "All."

TCGA database: TCGA is a comprehensive project including sequencing and pathological data of more than 30 types of human cancers. In this study, we downloaded the clinical data and mRNA-normalized count data of patients with LIHC from the TCGA database via the GDAC Firehose (gdac.broadinstitute.org). TCGA contains RNA-seq data for 374 primary HCCs and 50 adjacent normal solid liver tissue samples, and 364 of 374 patients with HCC had survival data.

ICGC database: ICGC is a global initiative to build a comprehensive catalog of mutational abnormalities in the major tumor (dcc.icgc.org). ICGC contains data from 84 worldwide cancer projects, including 11 molecular data types. In this study, we downloaded the LIHC sequencing-based gene expression (contains 232 tumor and 199 non-tumor cases) and clinical data (232 patients) of project "Liver Cancer-RIKEN, Japan."

GEO database: GEO is a public database that includes chips, second-generation sequencing, and high-throughput sequencing, which is uploaded by scientists worldwide. In this study, seven microarray expression datasets, including GSE102079, GSE164760, GSE121248, GSE25079, GSE14520, GSE55092, and GSE57895, containing expression data from HCC tumor and non-tumor samples and clinical data of GSE14520 (221 patients) downloaded from the GEO database (www.ncbi.nlm.nih.gov/geo/) were assessed. The platforms and samples of GEO series resources are summarized in Table S1.

UALCAN

UALCAN is an interactive web resource based on the TCGA database (7). It can be used to analyze the

association between transcriptional expression and relative clinicopathological parameters. Here, we analyzed the relationship between PPARG expression and *TP53* mutations, and the P value is calculated from the website. We downloaded the resulting images and included a statistical line for P<0.05*, P<0.01**, and P<0.001***.

Kaplan-Meier Plotter database analysis

Kaplan-Meier Plotter (8) (http://kmplot.com/analysis/) is an online database containing microarray gene expression data and survival information from public databases, such as the GEO and TCGA, that are similarly compatible for custom data analysis. We distributed the patient samples into high- and low-expression groups according to the best cutoff of PPARG expression. Additionally, we computed the hazard ratio (HR) with 95% confidence intervals and log-rank P value through Kaplan-Meier Plotter.

GO and KEGG analyses

Genes with a positive or negative correlation (cutoff P<0.05) were analyzed by GO and KEGG using the Database for Annotation, Visualization, and Integrated Discovery (DAVID) (https://david.ncifcrf.gov/). After downloading the results of GO [biological process (BP)] and KEGG enrichment, we used the Hiplot Online Tool (https://hiplot.com.cn/) to visualize data, create a circular bar-plot, Venn diagram, bubble diagram, and bar-plot gradient.

Timer2.0 database

Timer2.0 is a comprehensive resource for systematic analysis of immune infiltrates across diverse cancer types (http://timer.comp-genomics.org/) (9). Timer2.0 allows users to analyze immune infiltrations with six datasets—TIMER, CIBERSORT, quanTIseq, xCell, MCP-counter, and EPIC. As the EPIC algorithm requires no adjustment for the purity of the association analysis using the estimations from EPIC, in this study, we used the results of EPIC (10) that includes seven types of immune cells as follows: B cells, cancer-associated fibroblasts (CAFs), CD4+ T cells, CD8+ T cells, endothelial cells, macrophages, and natural killer (NK) cells.

Cell culture

HepG2 (SCSP-510, Shanghai Institute of Biochemistry and Cell Biology, China) was cultured in RPMI-1640 (Gibco, Germany) with 100 mg/mL streptomycin, 100 U/mL penicillin, and 10% Foetal Bovine Serum. After Cell was seeding to a 6-well plate or 8-well chamber slide for overnight, the culture medium was replaced with pioglitazone (PZG) or PZG and GW9662 or without drug addition medium for 24 h.

Quantitative polymerase chain reaction (qPCR)

After collecting HepG2 cell samples from 6-well plate, Total RNA was extracted using RNeasy Mini Kit (Qiagen, Germany). 3 μg of total RNA was reverse transcribed into cDNA using HiScript III RT SuperMix for qPCR (+gDNA wiper) (Vazyme, China). ChamQ Universal SYBR qPCR Master Mix (Vazyme, China) was used for qPCR. Primer details was attached in Table S2. PCR was carried out for 40 cycles under the following conditions: 10 s at 95 ℃ and 30 s at 60 ℃. By using the formula $2^{-\Delta\Delta CT}$ to normalized GAPDH mRNA, the relative fold change of mRNA expression is calculated. All experiments were repeated five times.

Immunofluorescence

After cell was cultured with PZG or GW9662 for 24 h in 8-well chamber slide, EdU was added to the medium and cultured for 1 hour. And EdU Cell Proliferation Kit (Sangon Biotech, China) was used to measure cell proliferation rate. The experimental procedure is based on the manual. The proliferating cells and all cells in each group were counted and the proliferating rate was calculated, and *t*-test to determine the statistical significance between groups. All experiments were repeated five times.

Workflow

First, we analyzed two websites with different datasets, including TIMER2.0 (9) (http://timer.comp-genomics.org/, Cancer Exploration, Gene_ED) and ONCOMINE (11) to investigate the differences in expression of PPARG mRNA in LIHC and normal tissues. Further, we downloaded the clinical and mRNA data of patients with LIHC from the TCGA, GEO, and ICGC database. The complete clinical and transcriptional data of 817 patients (TCGA-LIHC: 364, ICGC-LIRI-JP: 232, and GSE14520: 221) were included for the survival, immune, and enrichment analyses. Moreover, the relationship

between PPARG and HepG2 cell proliferation was verified in laboratory.

Statistical analysis

Statistical methods used in PPARG expression analysis include online results (TCGA, ONCOMINE), *t*-test (GEO,ICGC), and analysis of variance (tumor stage). All statistical results in survival analysis were calculated by Kaplan-Meiter Plotter. Genes associated with PPARG were calculated using Person method by R code and all statistical results in enrichment analysis were calculated by DAVID. Correlation between PPARG and immune cells were calculated using Person method by R code. All laboratory data were analyzed using *t*-test (*, P<0.05, **, P<0.01, ***, P<0.001.)

Results

PPARG mRNA expression levels in patients with HCC

To determine the differences in PPARG expression between tumor and normal tissues, the PPARG mRNA levels in tumor and normal tissues of multiple cancer types were analyzed using Timer2.0 and Oncomine databases. The analyses indicated that the expression of PPARG in liver cancer tissues was higher than that in normal tissues (*Figure 1A*,*1B*). Additionally, analyses of the GSE and ICGC databases showed similar results: PPARG mRNA was significantly overexpressed in GSE102079, GSE164760, GSE121248, GSE25079, GSE14520, GSE55092, GSE57895, and ICGC databases (*Figure 1C-1J*). The fold changes (1.06–1.945), P values (0.035–1.92E-34), and *t*-test from different data sources are shown in Table S3 (12-19). Further, we determined the association between mRNA expression of PPARG and the clinical stage and *TP53* mutation status in patients with HCC using RNA-seq and clinical data from the TCGA, ICGC and GSE14520 databases, and the UALCAN data mining website. The correlation analysis showed no significant difference in expression of PPARG in the TCGA and GSE14520 databases, however it was significant in the ICGC database (*Figure 1K-1M*). Conversely, the upregulation of PPARG was observed at Stage 4 in the ICGC database. These data suggest that PPARG mRNA levels do not change significantly with the clinical stage. Moreover, PPARG expression was significantly increased in the *TP53* mutation group of patients with HCC (*Figure 1N*), indicating that *TP53* mutation may be involved in the regulation of PPARG mRNA expression.

Prognostic significance of PPARG expression in patients with HCC

We investigated the prognostic significance of PPARG expression in patients with HCC using the Kaplan-Meier plotter (http://kmplot.com/analysis/). As shown in *Figure 2*, Kaplan-Meier plots demonstrated that high PPARG mRNA levels correlated with unfavorable overall survival (OS) [*Figure 2A*, hazard ration (HR) =1.8 (1.25 to –2.59), P=0.0014] and progression-free survival (PFS) [*Figure 2B*, HR =2.16 (1.37–3.4), P=0.00067], but not with recurrence-free survival (RFS) [*Figure 2C*, HR =0.78 (0.54–1.12), P=0.18] based on the TCGA database; similarly, they correlated with worse OS [*Figure 2D*, HR =2.91 (1.59–5.35), P=0.00029] in the ICGC database, and poorer OS [*Figure 2E*, HR =1.88 (1.22–2.9), P=0.0035] and RFS [*Figure 2F*, HR =1.52 (1.05–2.2), P=0.025] in the GSE14520 database. These results indicated that the mRNA expression of PPARG was significantly associated with prognosis in patients with HCC, and may be exploited as a useful biomarker for predicting HCC patient survival. Further, patients with HCC from these databases were distributed into low- or high-expression subgroups. We performed the chi-square test to study the correlation between PPARG expression and a panel of clinical features. As shown in *Table 1*, PPARG expression closely correlated with race (P=0.004) and neoplasm histologic grade (P=0.000962) in the TCGA; and with sex (P=0.023) and Liver Cancer Study Group of Japan (LCSGJ) stage (P=0.006) in the ICGC database. Furthermore, we investigated the association of OS with PPARG expression and the clinical characteristics of patients with HCC (*Table 2*). Overexpression of PPARG was associated with worse OS in men and women, and the results suggest that men with high PPARG had a higher risk of unfavorable OS in the three databases. In the TCGA database, PPARG expression significantly correlated with poor OS in patients from all races, alcohol consumption status (yes or no), hepatitis virus infection (no), all grade, and American Joint Committee on Cancer (AJCC) stage II; however, it did not correlate with OS of patients with AJCC stage I and vascular invasion. In the ICGC database, PPARG expression significantly correlated with poor OS in all LCSGJ stages and prior malignancy (yes or no). In the GSE14520, PPARG expression significantly correlated with poor OS in AJCC

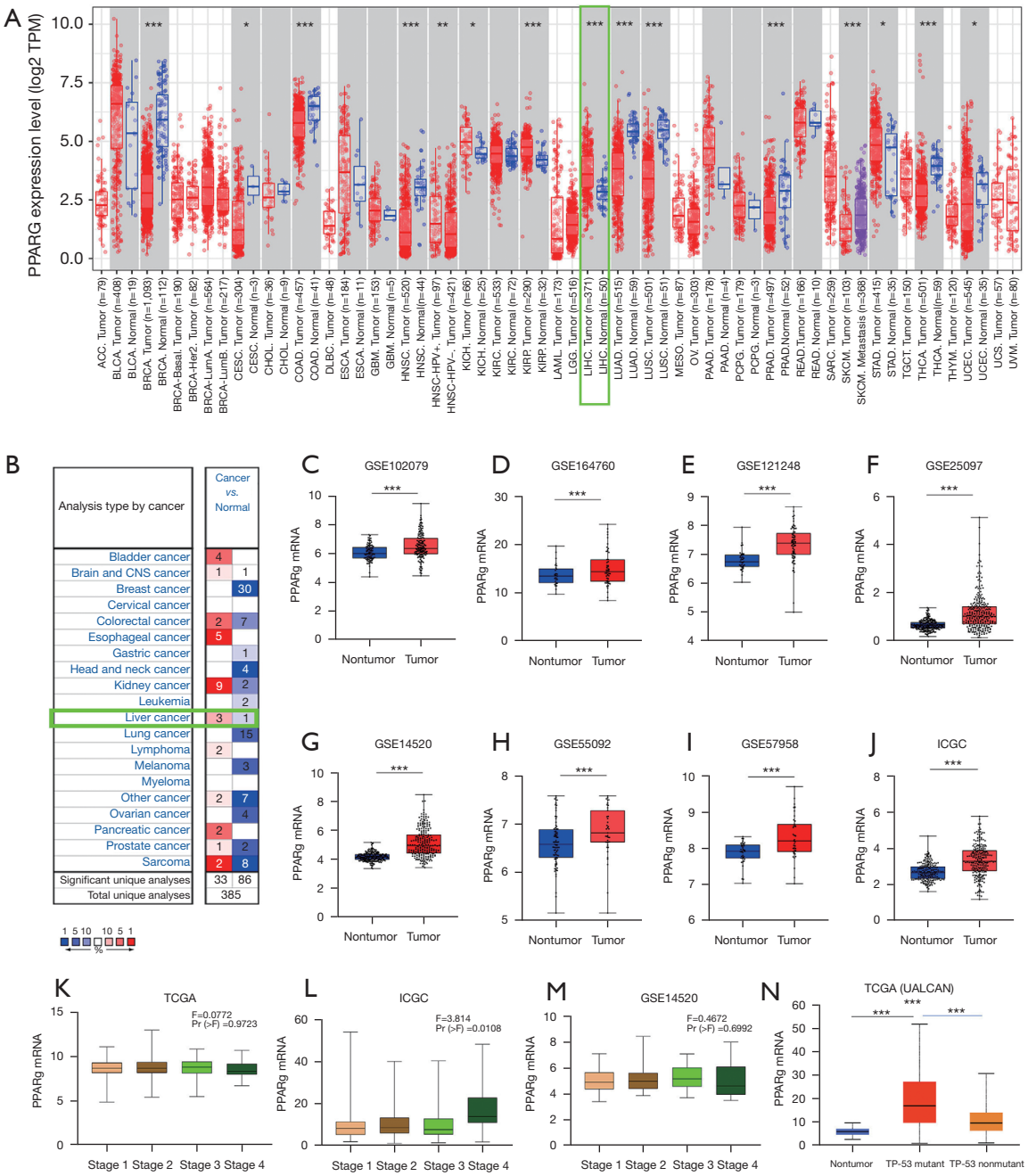

Figure 1 Expression characteristics of PPARG mRNA levels in patients with HCC. PPARG mRNA expression levels between nontumor and tumor tissues according to data of HCC patients in the (A) TCGA database (graph downloaded from timer2.0, as well as P value); (B) Oncomine database; GEO database (P value is obtained by the *t*-test) series including (C) GSE102079, (D) GSE164760, (E) GSE121248, (F) GSE25097, (G) GSE14520, (H) GSE55092, (I) GSE57598 and (J) ICGC database (project: LIRI-JP). Box plots were derived from correlation between PPARG expression and tumor stage [(K) TCGA, (L) ICGC, (M) GSE14520, P values were obtained by analysis of variance] and *TP53* mutation [(N) TCGA, graph downloaded from UALCAN, as well as P value]. *, P<0.05, **, P<0.01, ***, P<0.001. GEO, Gene Expression Omnibus dataset; GSE, Genomic Spatial Event; HCC, hepatocellular carcinoma; ICGC, International Cancer Genome Consortium; LIHC, liver hepatocellular carcinoma; PPARG, peroxisome proliferator-activated receptor gamma; TCGA, The Cancer Genome Atlas.

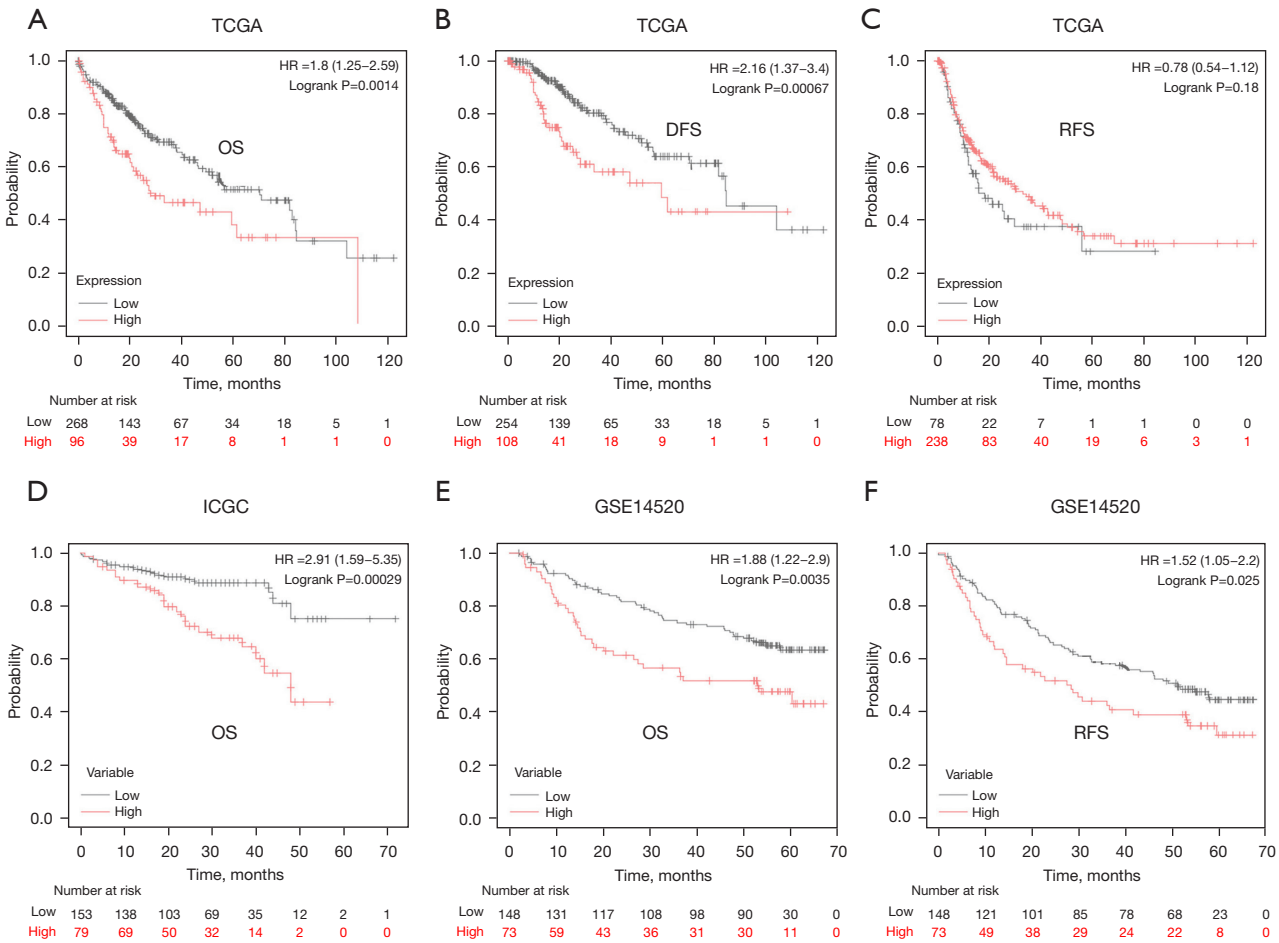

Figure 2 The prognostic value of mRNA levels of PPARG in HCC patients (Kaplan-Meier plotter). Plot showing the relationship between high expression (red) and low expression (black) of PPARG with (A) OS, (B) DFS, (C) RFS in TCGA database, (D) OS in the ICGC database, and (E) OS, (F) RFS in the GSE14520. HR and P values were calculated by Kaplan-Meier Plotter, P<0.05 with statistical significance. DFS, disease-free survival; HCC, hepatocellular carcinoma; HR, hazard ratio; ICGC, International Cancer Genome Consortium; OS, overall survival; PPARG, peroxisome proliferator-activated receptor gamma; RFS, recurrence-free survival; TCGA, The Cancer Genome Atlas.

stages I and IV, unlike AJCC stages II and III, and HBV status [chronic carrier (CC) or active viral replication chronic carrier (AVR-CC)]. All Kaplan-Meier plots based on the clinical characteristics of patients with HCC are shown in Figure S1, and the data are consistent with that in *Table 2*. Several factors can lead to inconsistency between databases; however, these results still suggest that PPARG expression impacts the prognosis of patients with HCC.

KEGG/GO biological process enrichment

To understand the underlying biological processes, we determined the correlation between PPARG and other genes in the three databases using Spearman's correlation coefficient, and values of P<0.05 were considered statistically significant. The genes were subsequently classified divided into two groups as follows: R>0 or R<0. The number of positively correlated genes was 3,647 in the TCGA, 6,000 in the ICGC, and 1,025 in the GSE14520. The top 20 GO (BP) and KEGG pathways enriched and positively correlated with genes in the three databases are shown as a circular bar plot (*Figure 3A,3B*); this plot shows several pathways associated with cancer process be enriched, such as RNA activity (rRNA processing, mRNA splicing,

Table 1 Characteristics of HCC patients between PPARG high and low groups

Variables		PPARG expression level		P value
		Low (%)	High (%)	
TCGA				
Age, years	≤50	55 (20.5)	21 (21.9)	0.78
	>50	213 (79.5)	75 (78.1)	
Gender	Female	88 (32.8)	30 (31.3)	0.776
	Male	18 (67.2)	66 (68.8)	
BMI	<18.5	14 (5.2)	7 (7.3)	0.692
	18.5–24.99	114 (42.5)	40 (41.7)	
	25–29.99	67 (25.0)	22 (22.9)	
	>30	53 (19.8)	14 (14.6)	
Race	White	146 (54.5)	35 (36.5)	0.004
	Black/Africa	10 (3.7)	7 (7.3)	
	Asian	102 (38.1)	53 (55.2)	
Hepatocarcinoma risk factors	Hepatitis virus infection	110 (41.0)	41 (42.7)	0.424
	Alcohol consumption	80 (29.9)	35 (36.5)	
	No risk	79 (29.5)	23 (24.0)	
Cancer status	With tumor	107 (40.0)	42 (43.8)	0.3477
	Tumor-free	151 (56.3)	47 (49.0)	
AJCC stage	I	128 (47.8)	42 (43.8)	0.466
	II	60 (22.4)	24 (25.0)	
	III	43 (16.0)	23 (24.0)	
	IV	15 (5.6)	5 (52.1)	
Neoplasm histologic grade	G1	48 (17.9)	7 (7.3)	0.000962
	G2	137 (51.1)	38 (40.0)	
	G3	73 (27.2)	44 (45.8)	
	G4	7 (2.6)	5 (5.2)	
Pathology_T_stage	T1	136 (50.7)	44 (45.8)	0.494
	T2	66 (24.6)	24 (25.0)	
	T3	48 (17.9)	24 (25.0)	
	T4	15 (5.6)	4 (4.2)	
Pathology_N_stage	N0	179 (66.8)	69 (71.9)	0.832
	N1	2 (0.7)	1 (1.0)	
Pathology_M_stage	M0	189 (70.5)	73 (76.0)	0.283
	M1	3 (1.1)	0 (0.0)	

Table 1 (*continued*)

Table 1 (*continued*)

Variables		PPARG expression level		P value
		Low (%)	High (%)	
Vascular invasion	Macro	10 (3.7)	5 (5.2)	0.621
	Micro	67 (25.0)	23 (24.0)	
	None	158 (59.0)	47 (49.0)	
ICGC				
Age, years	≤50	12 (7.8)	5 (6.3)	0.675
	>50	141 (92.2)	74 (93.7)	
Gender	Female	33 (21.6)	28 (35.4)	0.023
	Male	120 (78.4)	51 (64.6)	
LCSGJ stage	I	28 (18.3)	8 (10.1)	0.006
	II	70 (45.8)	36 (45.6)	
	III	49 (32.0)	22 (27.8)	
	IV	6 (3.9)	13 (16.5)	
GSE14520				
Age, years	≤50	79 (53.4)	33 (45.2)	0.253
	>50	69 (46.6)	40 (54.8)	
Gender	Female	21 (14.2)	9 (12.3)	0.704
	Male	127 (85.8)	64 (87.7)	
HBV viral status	CC	107 (72.3)	49 (67.1)	0.84
	AVR-CC	36 (24.3)	20 (27.4)	
	No risk	4 (2.7)	2 (2.7)	
AJCC stage	I	66 (44.6)	27 (37.0)	0.688
	II	51 (34.5)	26 (35.6)	
	III	18 (12.2)	12 (16.4)	
	IV	12 (8.1)	7 (9.6)	
Main tumor size (>5/≤5 cm)	Large	47 (31.8)	33 (45.2)	0.055
	Small	100 (67.6)	40 (54.8)	

HCC, hepatocellular carcinoma; PPARG, peroxisome proliferator-activated receptor gamma; BMI, body mass index; HBV, hepatitis B virus; AJCC, American Joint Committee on Cancer; ICGC, International Cancer Genome Consortium; AVR, active viral replication; CC, chronic carrier.

RNA splicing, nuclear-transcribed mRNA catabolic process, mRNA 3-end processing), cell division (cell division), cell-cell adhesion, and cell cycle (G1/S transition of mitotic cell cycle). Furthermore, 2,626 positively correlated genes were identified using a Venn diagram based on the condition that each gene appeared in two or more databases (2,239 genes in two databases and 387 genes in three database (*Figure 3C*). The bubble diagram and bar plot gradient of GO (BP) enrichment showed that rRNA processing, cell division, translation, translational initiation, mRNA splicing via spliceosome, mitotic nuclear division, nuclear-transcribed mRNA catabolic process, nonsense-mediated decay, viral transcription, signal recognition particle (SRP)-dependent translational protein targeting to membrane, and

Table 2 Correlation of PPARG mRNA expression a clinical prognosis in liver cancer with different clinicopathological factors by Kaplan-Meier plotter

Clinicopathological characteristics	Overall survival		
	N	Hazard radio	P value
TCGA-LIHC			
Sex			
Female	118	2.34 (1.31–4.15)	0.0027*
Male	246	1.58 (1–2.49)	0.047*
Race			
White	181	1.9 (1.2–3.02)	0.0058*
Asian	155	2.01 (1.11–3.65)	0.02*
Alcohol consumption			
Yes	115	2.29 (1.12–4.69)	0.019*
No	202	1.81 (1.12–2.9)	0.013*
Hepatitis virus			
Yes	150	0.71 (0.36–1.42)	0.33
No	167	2.4 (1.5–3.84)	0.00016*
Grade			
I	180	1.87 (1.04–3.33)	0.033*
II	90	2.35 (1.13-4.87)	0.018*
III	78	2.03 (1.09–3.78)	0.023*
AJCC stage			
I	55	2.11 (0.8–5.57)	0.12
II	174	1.82 (1.06–3.1)	0.026*
III	118	2.08 (1.13–3.84)	0.017
Vascular invasion			
None	203	0.68 (0.4–1.15)	0.15
Mirco	90	2.07 (0.95-4.48)	0.06
LIRI-JP			
Sex			
Female	61	6.27 (2–19.64)	0.00033*
Male	171	2.79 (1.12–6.94)	0.021*
LCSGJ stage			
II	106	7.64 (2.89–20.18)	1.90E-06*
III	71	3.04 (0.9–9.56)	0.045*
IV	19	0.21 (0.04–1.06)	0.038*

Table 2 (*continued*)

Table 2 (*continued*)

Clinicopathological characteristics	Overall survival		
	N	Hazard radio	P value
Prior malignancy			
Yes	30	15.2 (1.81–127.49)	0.00093*
No	202	2.54 (1.31–4.91)	0.0004*
GSE14520			
Sex			
Female	30	6.43 (1.52–27.16)	0.0038*
Male	191	1.63 (1.03–2.58)	0.033*
HBV viral status			
CC	156	1.66 (0.97–2.83)	0.06
AVR-CC	56	1.72 (0.96–3.82)	0.18
AJCC stage			
I	93	2.36 (0.99–5.61)	0.045*
II	77	1.9 (0.94–3.83)	0.067
III	30	0.63 (0.24–1.63)	0.34
IV	19	10.17 (1.27–81.71)	0.0078*

*, indicate P<0.05. HCC, hepatocellular carcinoma; PPARG, peroxisome proliferator-activated receptor gamma; BMI, body mass index; HBV, hepatitis B virus; AJCC, American Joint Committee on Cancer; ICGC, International Cancer Genome Consortium; AVR, active viral replication; CC, chronic carrier; TCGA, The Cancer Genome Atlas; LIHC, liver hepatocellular carcinoma.

cytoplasmic translation were the most enriched biological processes (*Figure 3D,3E*). The bubble diagram and bar plot gradient of KEGG showed enrichment of ribosome, RNA transport, spliceosome, ubiquitin-mediated proteolysis, cell cycle, ribosome biogenesis in eukaryotes, pyrimidine metabolism, RNA degradation, shigellosis, and basal transcription factors (*Figure 3F,3G*). The results of the positively correlated genes showed that high PPARG may lead to more active rRNA, mRNA activity, cell division, and cell cycle activity. Additionally, we performed an enrichment analysis for the negatively correlated genes. The number of negatively correlated genes was 3,796 in the TCGA, 1,446 in the ICGC, and 1,326 in the GSE14520. The top 20 GO (BP) and KEGG pathways enriched and negatively correlated with genes in the three databases are shown as a circular bar plot (*Figure 3H,3I*). The biological processes enriched were metabolically related pathways and some biological processes associated with severity of HCC, such as cell adhesion, regulation of complement activation, and complement activation alternative pathway. Furthermore, 1,241 negatively correlated genes were identified using a Venn diagram based on the condition that each gene appeared in two or more databases (1,051 genes in two databases and 190 genes in three database, *Figure 3J*). The bubble diagram and bar plot gradient of GO (BP) enrichment showed that Oxidation-reduction process, cell adhesion, metabolic process, extracellular matrix organization, xenobiotic metabolic process, negative regulation of endopeptidase activity, steroid metabolic process, regulation of complement activation, branched-chain amino acid catabolic process, complement activation, alternative pathway (*Figure 3K,3L*). The bubble diagram and bar plot gradient of KEGG showed enrichment of metabolic pathways, Biosynthesis of antibiotics, complement and coagulation cascades, carbon metabolism, valine, leucine and isoleucine degradation, tryptophan metabolism, steroid hormone biosynthesis, fatty acid degradation, Glycine, serine and threonine metabolism, beta-alanine

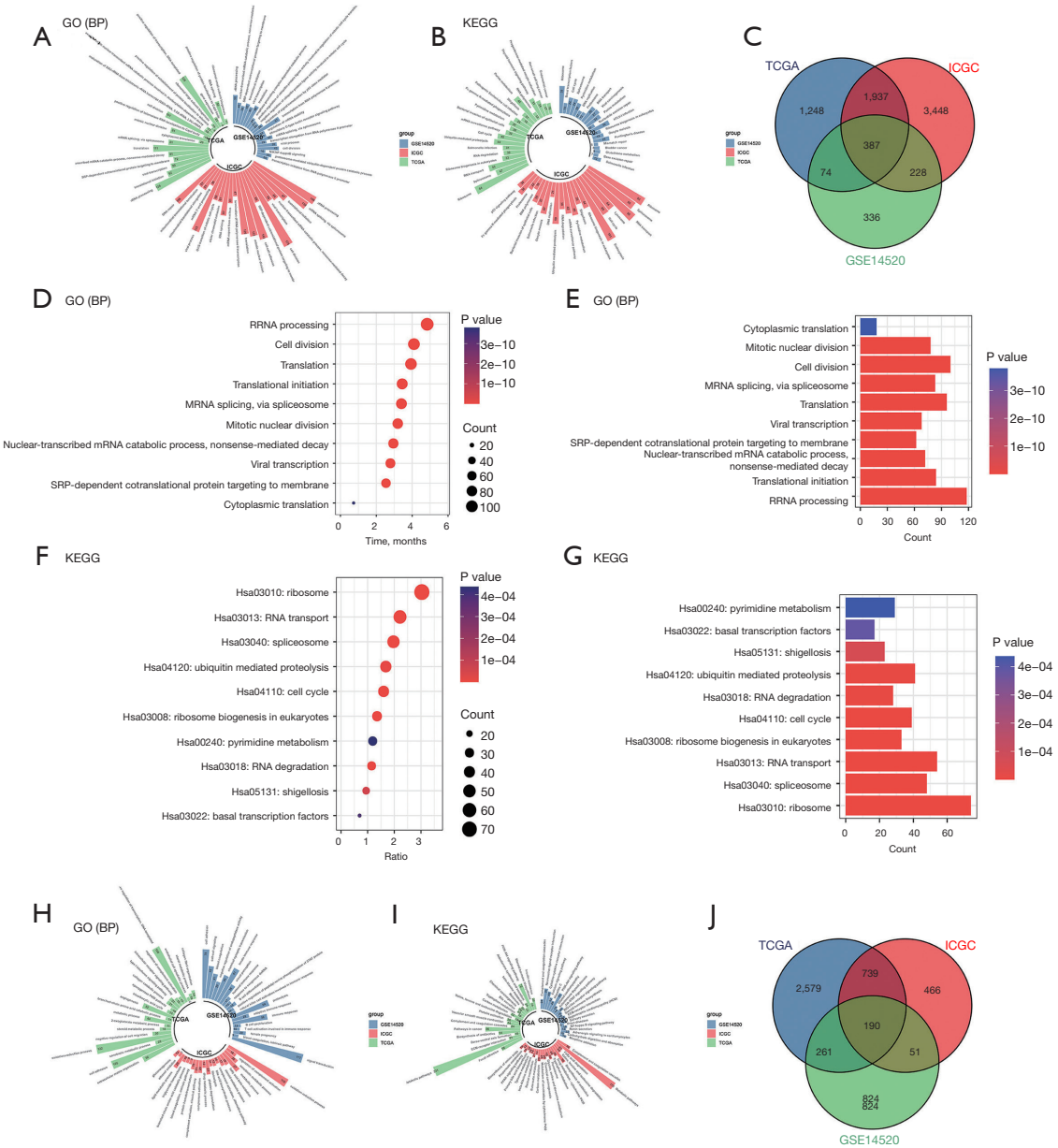

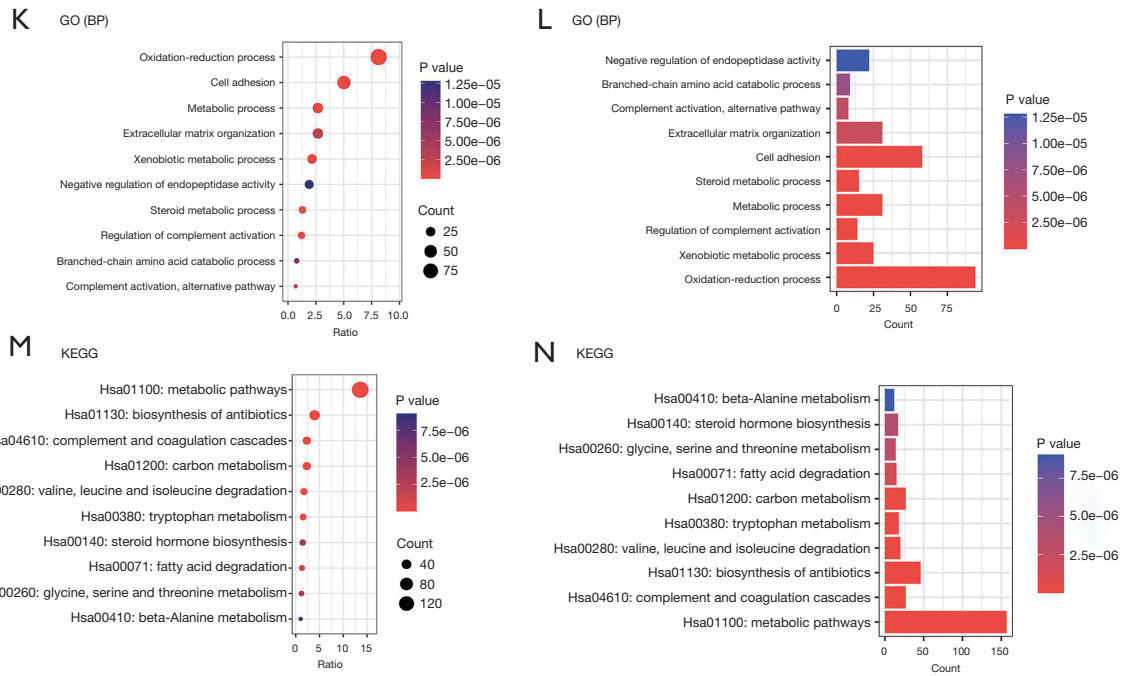

Figure 3 KEGG/GO (BP) enrichment. Positive correlation genes enrichment is shown in the: (A) circular bar plot of three databases [GO (BP) enrichment analysis]: (B) circular bar plot of three databases (KEGG enrichment analysis); (C) Venn diagram of three databases; (D) bubble diagram of common genes [GO (BP) enrichment analysis]; (E) bar plot gradient of common genes [GO (BP) enrichment analysis]; (F) bubble diagram of common genes (KEGG enrichment analysis); and (G) bar plot gradient of common genes (KEGG enrichment analysis). (H-N) Show negative correlation genes enrichment. All P values were calculated by DAVID. BP, biological process; DAVID, Database for Annotation, Visualization, and Integrated Discovery; GO, Gene Ontology; ICGC, International Cancer Genome Consortium; KEGG, Kyoto Encyclopedia of Genes and Genomes; SRP, signal recognition particle; TCGA, The Cancer Genome Atlas.

metabolism (*Figure 3M,3N*).

Association between PPARG and immune system

Because PPARG was possibly related to the downregulation of complement activity, the correlation between PPARG expression and complement system was further analyzed using the three databases. The results showed a negative correlation of PPARG with C1r, C1s, C2, C3, C5, C6 and C7, and the mean difference (all complements were lower in the high group than the low group) with the forest plot between the high and low PPARG groups (*Table S4*). Thus, the data showed that higher PPARG levels were associated with lower levels of the complement system. Furthermore, we calculated the immune cell infiltration EPIC in the three databases. The results from all the three databases were consistent, suggesting a negative correlation between PPARG and macrophage infiltration [*Figure 4A-4C*; TCGA (R=–0.17, P=0.00086), ICGC (R=–0.18, P=0.0075), and GSE14520 (R=–0.3, P=5.2e-6)] (*Figure 4A-4C*). In the TCGA database, PPARG also showed a negative correlation with CAFs (R=–0.13, P=0.014) and endothelial cells (R=–0.2, P=9.8e-5), and a positive correlation with CD8+ T cells (R=0.13, P=0.011). Meanwhile, PPARG was negatively correlated with B cells (R=–0.14, P=0.039), CAF (R=–0.16, P=0.015), and endothelial cells (R=–0.28, P=2.5e-5) in the GSE14520. Further, the Kaplan-Meier curves suggested that low PPARG expression in enriched macrophages was associated with favorable prognosis in patients with HCC (Figure S2). These data suggest that high levels of PPARG inhibit complement levels and immune infiltration that are associated with poor prognosis.

Association between PPARG and HepG2 proliferation

Enrichment results suggested that PPARG may be involved in the regulation of cell cycle. We tested this biological process in human hepatocellular carcinoma cells (HepG2)

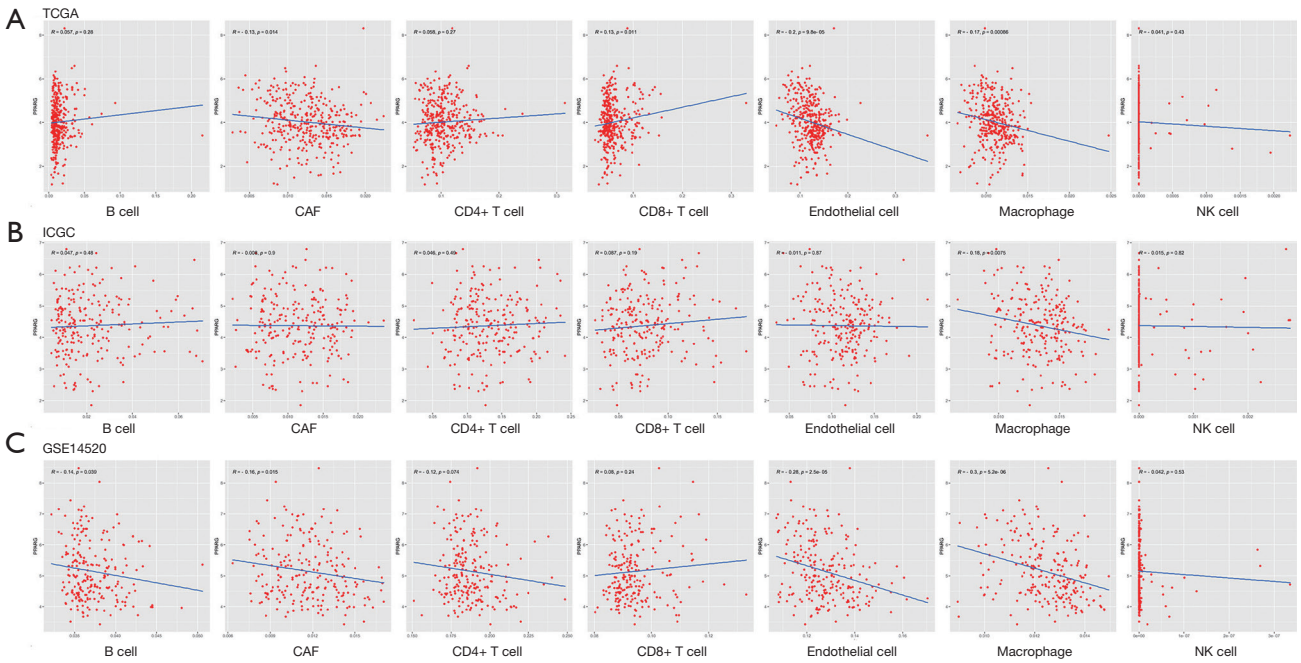

Figure 4 PPARG expression correlated with immune infiltration based on EPIC algorithm. Seven types of immune cells were included. (A) correlation between of PPARG and B cell, CAF, CD4+T cell, CD8+T cell, Endothelial cell, Macrophage, and NK cell infiltration in TCGA database. (B) Correlation between of PPARG and infiltration of the seven immune cells in the ICGC database; (C) correlation between of PPARG and infiltration of the seven immune cells in the GSE14520. R and P values were calculated using Pearson method by R language. P<0.05 with statistical significance. CAF, cancer-associated fibroblast; ICGC, International Cancer Genome Consortium; NK, natural killer; PPARG, peroxisome proliferator-activated receptor gamma; TCGA, The Cancer Genome Atlas.

by using pioglitazone (PZG, PPARG agonist) and GW9662 (PPARG inhibitor). qPCR results show that PZG inhibit the expression of CCND1, CCND2, and CDK4 while GW9662 eliminated this effect (*Figure 5A-5D*). And we determine the effect of PPARG on cell proliferation rates through Immunofluorescence, showing the consistent results with qPCR that PZG inhibits the proliferation of HepG2 and GW9662 has the opposite effect (*Figure 5E,5F*). These results support the role of PPARG in cell proliferation of HepG2 and suggest that PPARG could be used as a therapeutic target for liver cancer.

Discussion

PPARG involved in several biological process, such as energy metabolism, cellular development, differentiation, and immune response (2-6). Previous studies found PPARG playing an anti-inflammatory role and preventing the occurrence of liver cancer (3-5). And our group also found PPARG to negatively correlate with the inflammatory response in NAFLD (6). Moreover, simvastatin inhibits tumor growth by suppressing the hypox inducible factor 1-α/PPARG/Pyruvate Kinase M2 axis (20). However, the role of PPARG in HCC remains unknown. Before further studying the role of PPARG in HCC, it is necessary to understand the possible prognostic effects of PPARG in HCC patients and the underlying mechanisms.

In this study, we analyzed the clinical and prognostic significance of PPARG mRNA expression, as well as its role in immunity, using the TCGA, ICGC, and GSE databases. For the first time, we discovered a high expression of PPARG mRNA in HCC tissues from the TCGA, ICGC, and seven GSE datasets. We found that expression of PPARG was almost independent of the clinical stage (statistically significant only in the ICGC database at stage IV), although it was strongly correlated with *TP53* mutation. The Kaplan-Meier plot showed that patients with HCC with high PPARG expression had poor OS, consistently in the three databases. The KEGG/GO (BP) enrichment analysis using the genes demonstrating a significant negative or positive correlation with PPARG showed the upregulation of rRNA, mRNA activity, cell

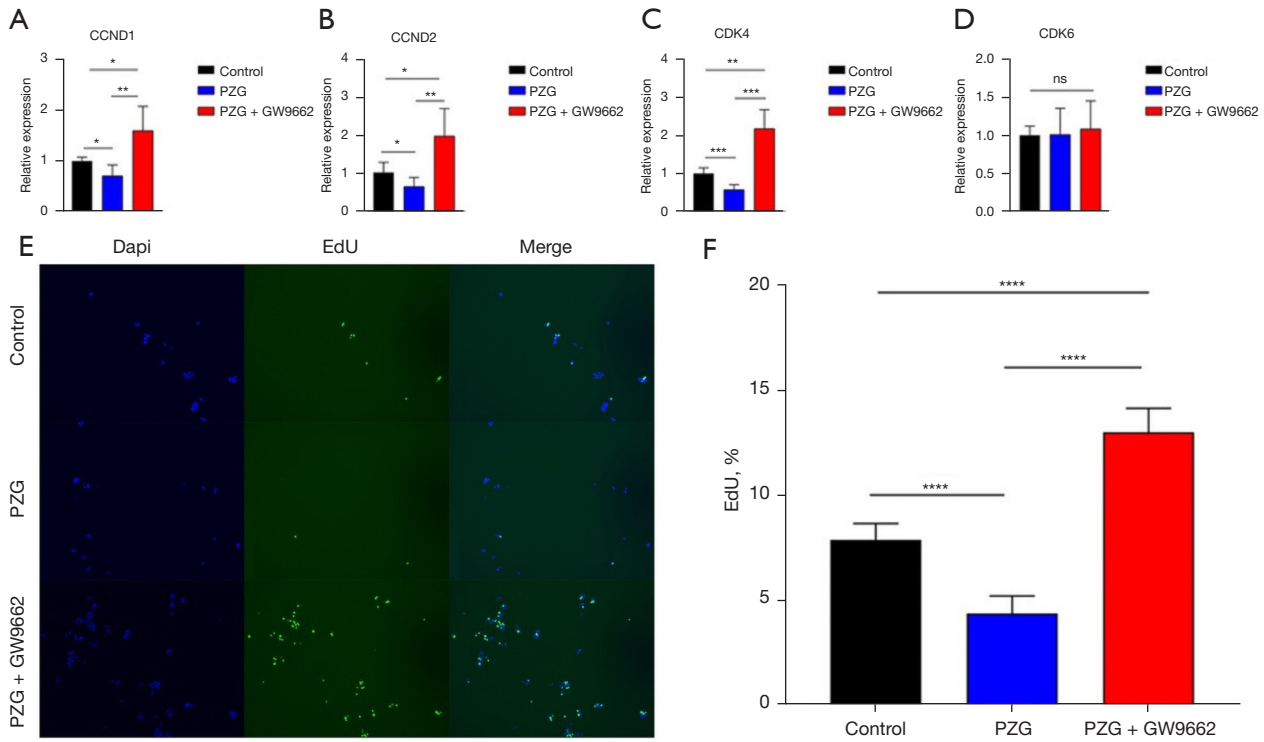

Figure 5 The relationship between PPARG and cell proliferation verified by qPCR and immunofluorescence. qPCR: (A) CCND1. (B) CCND2. (C) CDK4. (D) CDK6. (E) Immunofluorescence in three group (Control, PZG, and PZG with GW9662). (F) EdU/Dapi percent. *, P<0.05; **, P<0.01; ***, P<0.001; ****, P<0.0001. ns, no significant; PPARG, peroxisome proliferator-activated receptor gamma; qPCR, quantitative polymerase chain reaction; PZG, pioglitazone.

division and cell cycle, and downregulation of complement system, cell adhesion and coagulation cascades. After that, we found a negative correlation between the complement system and PPARG; similarly, we also observed a significant difference between the high and low groups, and in immune infiltration (especially macrophages). To the best of our knowledge, the present analyses provide novel insights into the prognostic role of PPARG, its potential biological processes, and its role in tumor immunology in HCC.

Whether PPARγ activation worsens or alleviates hepatic damage is still not completely clear (21). However, previous studies have suggested that PPARG expression is upregulated in obese patients and contributes to hepatic steatosis (22,23), while some studies focusing on the pre-disease conditions of liver cancer, such as NAFLD, non-alcoholic steatohepatitis and liver cirrhosis, identified PPARG to have beneficial effects (5,14,16,20), which may be due to the anti-inflammatory activity of PPARG thereby suppressing the occurrence of liver cancer. In a previous study by our group, we found a negative correlation between PPARG and inflammatory response (6). However, there is limited information about the clinical and prognostic roles of PPARG in liver cancer.

Finally, we tested the relationship between PPARG and HCC cell proliferation. Enrichment results suggested that PPARG may be involved in regulating the proliferation of HCC cells. And both results of qPCR and immunofluorescence supports it, which means that PPARG can also be used as a therapeutic target for HCC.

HCC has a high morbidity and mortality rate, with only 10% five-year survival. Therefore, the survival time of patients wth HCC is an important part to judge the prognostic characteristics. In this study, we systematically explored the association between high PPARG expression and survival in three reliable data sources. The results show that high PPARG expression is highly correlated with poor OS in patients with HCC compared to those with low PPARG expression; thus, PPARG may be a candidate biological indicator and drugs that inhibit or stimulate PPARG may help to study the disease mechanisms of liver

cancer or extend life expectancy in patients.

Previous study suggest that PPARG agonism indirectly inhibits hepatic macrophage infiltration (24), consistent with the present study results. We observed that PPARG expression was negatively correlated with macrophages in HCC tissues. This result may be consistent with that of macrophage infiltration; however, it can have adverse consequences on immune escape in HCC, along with downregulation of the complement system.

In general, our study presents a target gene: PPARG to the research about HCC. Based on the result through bioinformatics analysis in HCC patients from multiple database, we found that PPARG is associated with poor prognosis and low levels of complement and immune infiltration, which shows a possible explanation that high level of PPARG contribute to evade the immune system in HCC. And the results in hepG2 cell show the association between PPARG and cell proliferation through cyclin, and it could be a direction to development drug targeting PPARG to limit the growth of HCC.

This study has a few limitations. First, to avoid bias from single data, we analyzed three reliable databases (TCGA, ICGA, and GEO databases), which also conferred heterogeneity on the results. Additionally, we could not combine data from these databases to obtain consistent results; in most conditions, we analyzed each database individually and attempted to find common characteristics, and this limits the application of this study in clinical practice. Second, inconsistencies in survival data made it difficult to perform a meta-analysis of survival; however, results from all databases support the fact that PPARG predicts a poor prognosis. Finally, although we explored the biological processes of PPARG in HCC through enrichment analysis and the relationship between PPARG and liver cell proliferation through laboratory, the detailed mechanism associating PPARG expression with HCC progression requires further biomedical validations, and further studies are needed to support the prognostic and immunological values of PPARG. Nevertheless, this study is encouraging and noteworthy in the field of identifying promising prognostic biomarkers for HCC.

Acknowledgments

Useful support given by Dr. Han Huang is acknowledged.
Funding: None.

Footnote

Reporting Checklist: The authors have completed the MDAR reporting checklist. Available at https://tcr.amegroups.com/article/view/10.21037/tcr-21-2853/rc

Conflicts of Interest: All authors have completed the ICMJE uniform disclosure form (available at https://tcr.amegroups.com/article/view/10.21037/tcr-21-2853/coif). The authors have no conflicts of interest to declare.

Ethical Statement: The authors are accountable for all aspects of the work in ensuring that questions related to the accuracy or integrity of any part of the work are appropriately investigated and resolved. The study was conducted in accordance with the Declaration of Helsinki (as revised in 2013).

References

1. Sung H, Ferlay J, Siegel RL, et al. Global Cancer Statistics 2020: GLOBOCAN Estimates of Incidence and Mortality Worldwide for 36 Cancers in 185 Countries. CA Cancer J Clin 2021;71:209-49.
2. Cheng HS, Tan WR, Low ZS, et al. Exploration and Development of PPAR Modulators in Health and Disease: An Update of Clinical Evidence. Int J Mol Sci 2019;20:5055.
3. Pawlak M, Lefebvre P, Staels B. Molecular mechanism of PPARα action and its impact on lipid metabolism, inflammation and fibrosis in non-alcoholic fatty liver disease. J Hepatol 2015;62:720-33.
4. Gross B, Pawlak M, Lefebvre P, et al. PPARs in obesity-induced T2DM, dyslipidaemia and NAFLD. Nat Rev Endocrinol 2017;13:36-49.
5. Luo W, Xu Q, Wang Q, et al. Effect of modulation of PPAR-γ activity on Kupffer cells M1/M2 polarization in

the development of non-alcoholic fatty liver disease. Sci Rep 2017;7:44612.
6. Zhang Y, Wu B, Zhang H, et al. Inhibition of MD2-dependent inflammation attenuates the progression of non-alcoholic fatty liver disease. J Cell Mol Med 2018;22:936-47.
7. Chandrashekar DS, Bashel B, Balasubramanya SAH, et al. UALCAN: A Portal for Facilitating Tumor Subgroup Gene Expression and Survival Analyses. Neoplasia 2017;19:649-58.
8. Lánczky A, Nagy Á, Bottai G, et al. miRpower: a web-tool to validate survival-associated miRNAs utilizing expression data from 2178 breast cancer patients. Breast Cancer Res Treat 2016;160:439-46.
9. Li T, Fu J, Zeng Z, et al. TIMER2.0 for analysis of tumor-infiltrating immune cells. Nucleic Acids Res 2020;48:W509-14.
10. Racle J, de Jonge K, Baumgaertner P, et al. Simultaneous enumeration of cancer and immune cell types from bulk tumor gene expression data. Elife 2017;6:26476.
11. Rhodes DR, Yu J, Shanker K, et al. ONCOMINE: a cancer microarray database and integrated data-mining platform. Neoplasia 2004;6:1-6.
12. Alam H, Li N, Dhar SS, et al. HP1γ Promotes Lung Adenocarcinoma by Downregulating the Transcription-Repressive Regulators NCOR2 and ZBTB7A. Cancer Res 2018;78:3834-48.
13. Mah WC, Thurnherr T, Chow PK, et al. Methylation profiles reveal distinct subgroup of hepatocellular carcinoma patients with poor prognosis. PLoS One 2014;9:e104158.
14. Shimada S, Mogushi K, Akiyama Y, et al. Comprehensive molecular and immunological characterization of hepatocellular carcinoma. EBioMedicine 2019;40:457-70.
15. Ivanovska I, Zhang C, Liu AM, et al. Gene signatures derived from a c-MET-driven liver cancer mouse model predict survival of patients with hepatocellular carcinoma. PLoS One 2011;6:e24582.
16. Chiyonobu N, Shimada S, Akiyama Y, et al. Fatty Acid Binding Protein 4 (FABP4) Overexpression in Intratumoral Hepatic Stellate Cells within Hepatocellular Carcinoma with Metabolic Risk Factors. Am J Pathol 2018;188:1213-24.
17. Pinyol R, Torrecilla S, Wang H, et al. Molecular characterisation of hepatocellular carcinoma in patients with non-alcoholic steatohepatitis. J Hepatol 2021;75:865-78.
18. Wang SM, Ooi LL, Hui KM. Identification and validation of a novel gene signature associated with the recurrence of human hepatocellular carcinoma. Clin Cancer Res 2007;13:6275-83.
19. Roessler S, Jia HL, Budhu A, et al. A unique metastasis gene signature enables prediction of tumor relapse in early-stage hepatocellular carcinoma patients. Cancer Res 2010;70:10202-12.
20. Feng J, Dai W, Mao Y, et al. Simvastatin re-sensitizes hepatocellular carcinoma cells to sorafenib by inhibiting HIF-1α/PPAR-γ/PKM2-mediated glycolysis. J Exp Clin Cancer Res 2020;39:24.
21. Cariello M, Piccinin E, Moschetta A. Transcriptional Regulation of Metabolic Pathways via Lipid-Sensing Nuclear Receptors PPARs, FXR, and LXR in NASH. Cell Mol Gastroenterol Hepatol 2021;11:1519-39.
22. Gavrilova O, Haluzik M, Matsusue K, et al. Liver peroxisome proliferator-activated receptor gamma contributes to hepatic steatosis, triglyceride clearance, and regulation of body fat mass. J Biol Chem 2003;278:34268-76.
23. Pettinelli P, Videla LA. Up-regulation of PPAR-gamma mRNA expression in the liver of obese patients: an additional reinforcing lipogenic mechanism to SREBP-1c induction. J Clin Endocrinol Metab 2011;96:1424-30.
24. Lefere S, Puengel T, Hundertmark J, et al. Differential effects of selective- and pan-PPAR agonists on experimental steatohepatitis and hepatic macrophages ☆ . J Hepatol 2020;73:757-70.

Cite this article as: Wang C, Yu S, Qian R, Chen S, Dai C, Shan X. Prognostic and immunological significance of peroxisome proliferator-activated receptor gamma in hepatocellular carcinoma based on multiple databases. Transl Cancer Res 2022;11(7):1938-1953. doi: 10.21037/tcr-21-2853

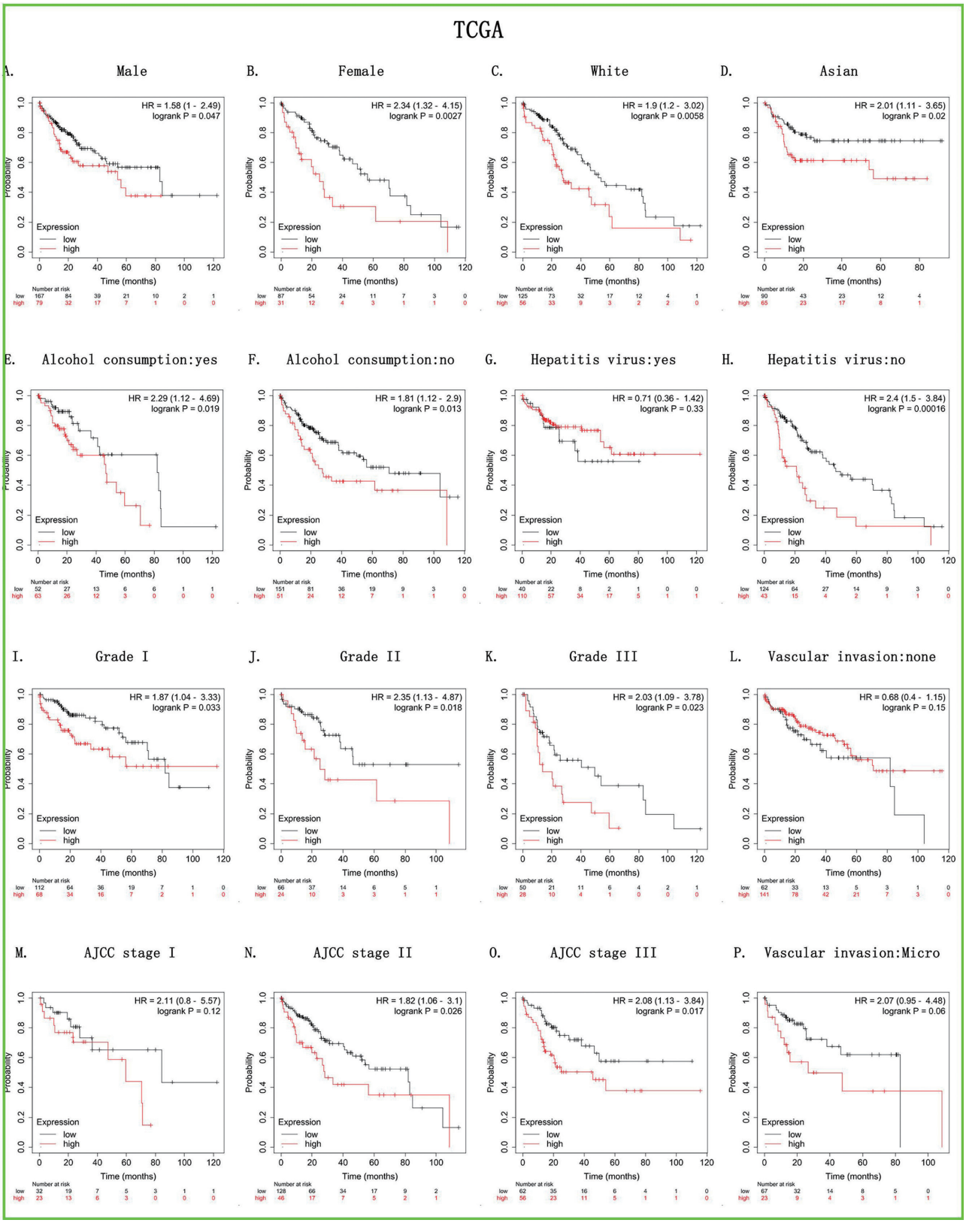

https://dx.doi.org/10.21037/tcr-21-2853

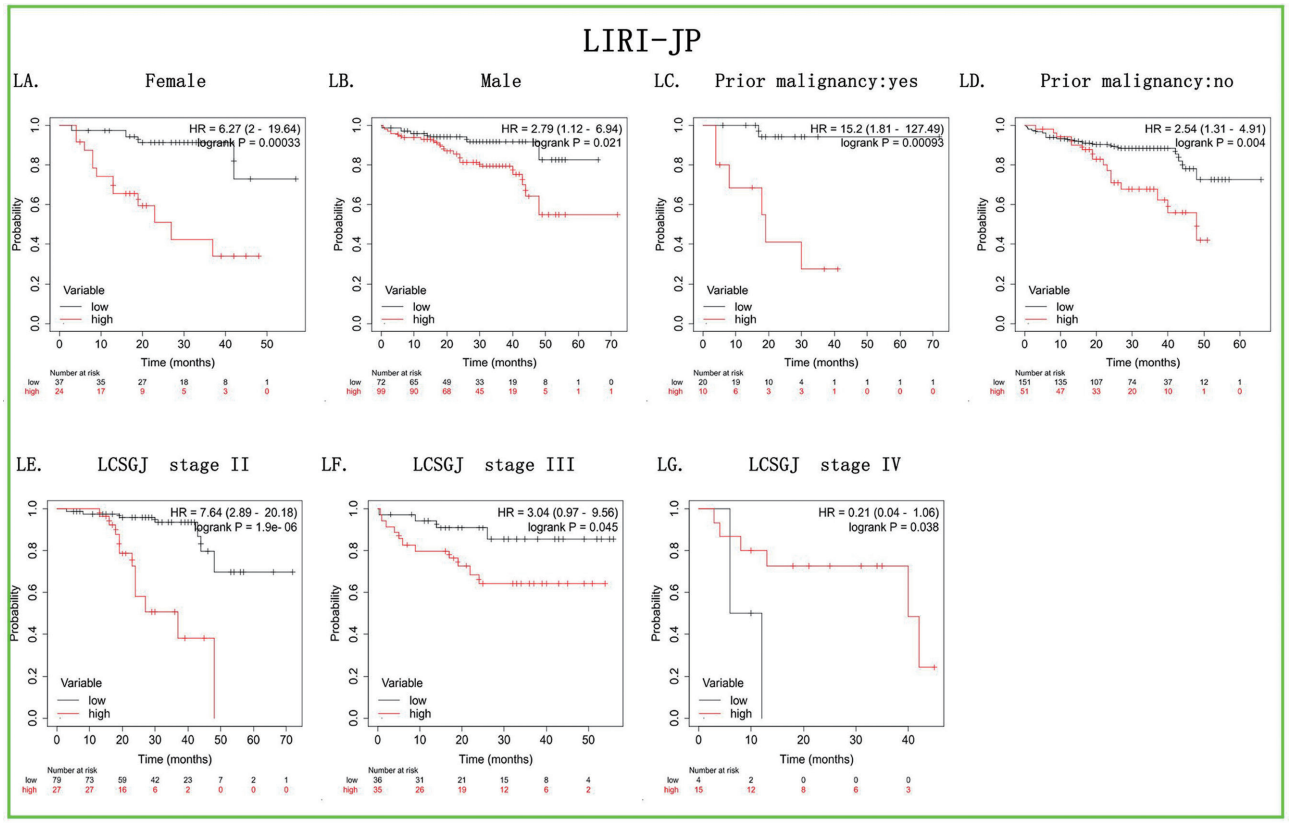

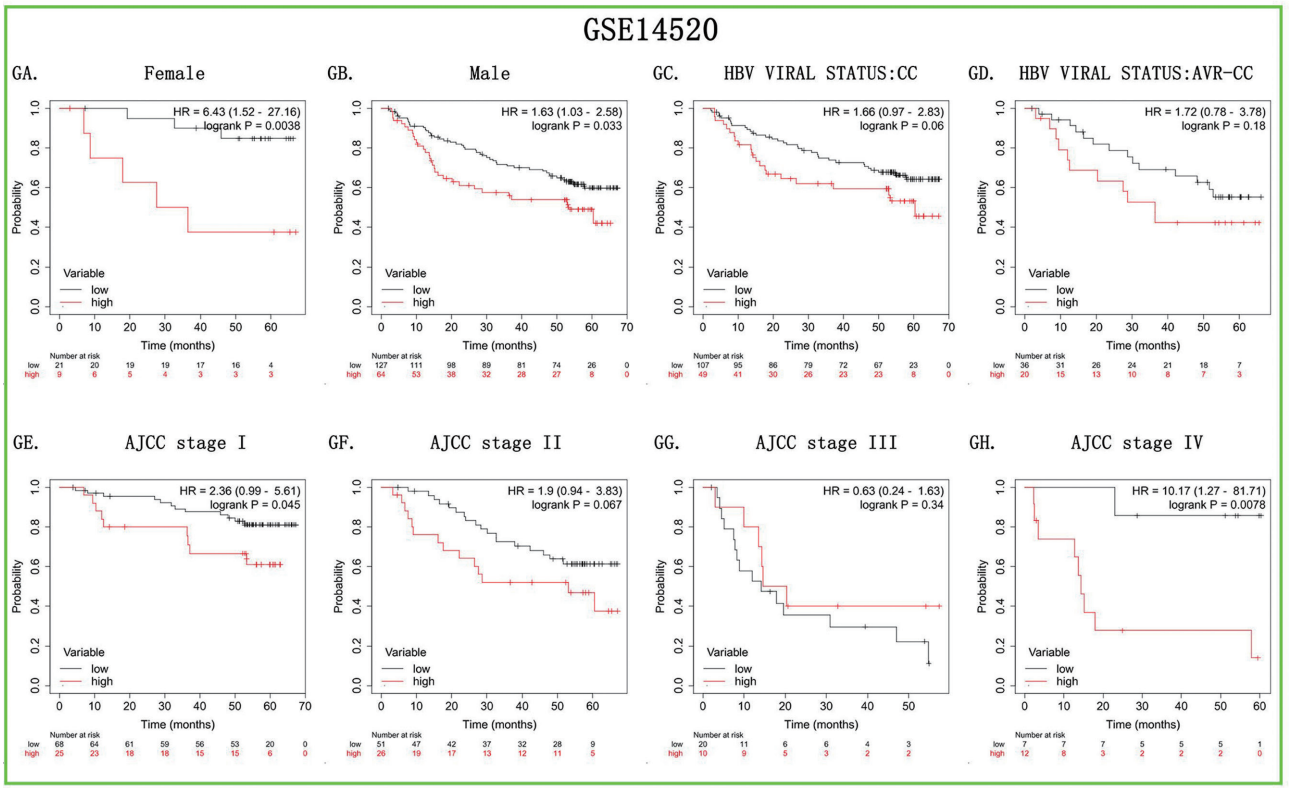

Figure S1 Subgroup analyses of overall survival comparison in HCC patients by Kaplan-Meier ploter. From the TCGA database: (A, B) sex; (C, D) race; (E, F) alcohol consumption; (G, H) hepatits virus; (L-K) grade; (M-0) AJCC stage; (L, P) vascular invasion. From the ICGC database: (LA, LB) sex; (LC, LD) prior malignancy; (LE-LG) LCSGJ stage.From the GSE14520: (GA, GB) sex, (GC, GD) HBV viral status, (GE-GH) AJCC stage. HR and P values were calculated by Kaplan-Meier Plotter, P<0. 05 with statistical significance. AJCC, American Joint Committee on Cancer; HBV, hepatitis B virus; HCC, hepatocellular carcinoma; HR, hazard ratio; ICGC, International Cancer Genome Consortium; LCSGJ, Liver Cancer Study Group of Japan; TCGA, The Cancer Genome Atlas.

https://dx.doi.org/10.21037/tcr-21-2853

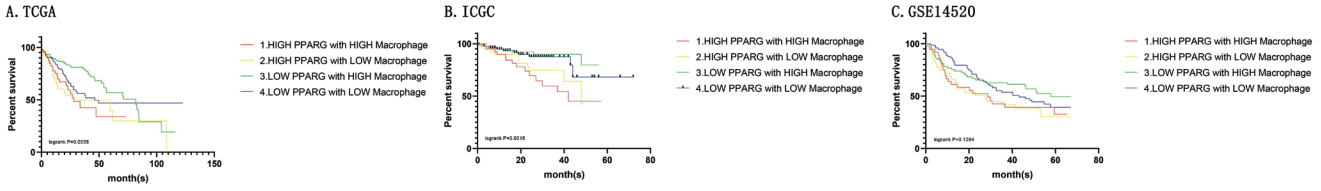

Figure S2 Kaplan-Meier plot of High or low PPARG expression with High or low Macrophage infiltration. (A) TCGA, (B) ICGC, (C) GSE14520. P value was calculated by GraphPad Prism8. ICGC, International Cancer Genome Consortium; PPARG, peroxisome proliferator-activated receptor gamma; TCGA, The Cancer Genome Atlas.

Table S1 Details of GEO series included in this analysis.

GEO series	Contributor (s)	Pre disease	Nontumor	Tumor	Platform
GSE102079	Norimichi, Chiyonobu *et al.*, 2018	unknown	91	152	Affymetrix Human Genome U133 Plus 2.0 Array
GSE164760	Josep, M, Llovet *et al.*, 2021	NASH	29	53	Affymetrix Human Genome U219 Array
GSE121248	Hui KM, 2018	HBV	37	70	Affymetrix Human Genome U133 Plus 2.0 Array
GSE25097	Chunsheng Zhang, 2011	unknown	243	268	Rosetta/Merck Human RSTA Affymetrix 1.0 microarray, Custom CDF
GSE14520#	Xin Wei Wang, 21010	unknown	220	225	Affymetrix HT Human Genome U133A Array
GSE55092	Michael, Kew *et al.*, 2014	unknown	39	81	Affymetrix Human Genome U133 Plus 2.0 Array
GSE57958	Lee, Guat Lay, Caroline, 2014	unknown	39	39	Illumina HumanHT-12 V4.0 expression beadchip

#GSE14520 contains clinical data.

Table S2 primer list

Gene symbol	Forward Primer(5'→3')	Reverse Primer(5'→3')
GAPDH	GGAGCGAGATCCCTCCAAAAT	GGCTGTFTGTCATACTTCTCATGG
CCND1	GCTGCGAAGTGGAAACCATC	CCTCCTTCTGCACACATTTGAA
CCND2	ACCTTCCGCAGTGCTCCTA	CCCAGCCAAGAAACGGTCC
CDK4	ATGGCTACCTCTCGATATGAGC	CATTGGGGACTCTCACACTCT
CDK6	GCTGACCAGCAGTACGAATG	GCACACATCAAACAACCTGACC

Table S3 Significant changes of PPARG expression in transcription level between HCC and normal liver tissues.

Data source	Types of HCC VS liver	Fold change	P value	*T*-test
Oncomine	Hepatocellular Carcinoma (Roessler Liver2)	1.945	1.92E-34	14.087
	Hepatocellular Carcinoma (Roessler Liver1)	1.655	8.77E-4	3.503
GEO				
GSE112791	Hepatocellular Carcinoma	1.11	7E-4	4.026
GSE57958	Hepatocellular Carcinoma	1.06	1E-4	4.103
GSE25097	Hepatocellular Carcinoma	1.7	1.23E-27	12.01
GSE102079	Hepatocellular Carcinoma	1.08	1E-6	4.94
GSE164760	Hepatocellular Carcinoma	1.10	0.035	2.146
GSE121248	Hepatocellular Carcinoma	1.08	9.97E-8	5.724
GSE14520	Hepatocellular Carcinoma	1.243	4.79E-34	14.055
ICGC(LIRI-JP)	Hepatocellular Carcinoma	1.238	1.3833E-18	9.217

HCC, hepatocellular carcinoma; PPARG, PPARG peroxisome proliferator activated receptor gamma.

https://dx.doi.org/10.21037/tcr-21-2853

Table S4 correlation between PPARG expression and complement as well as the mean difference of complement between High and Low PPARG expression group

Complement	Database	Cor	P	mean difference [95%CI]	Forest plot (mean difference)
C1r	TCGA	-0.213278887	***	-0.66 [-0.95, -0.37]	
	ICGC	-0.194087878	**	-0.78 [-1.10, -0.46]	
	GSE14520	0.256029761	***	-0.62 [-0.95, -0.28]	
C1s	TCGA	-0.213897117	***	-0.75 [-1.04, -0.46]	
	ICGC	-0.166287822	*	-0.78 [-1.11, -0.45]	
	GSE14520	0.321975925	***	-0.63 [-0.94, -0.32]	
C2	TCGA	0.096270606	0.067	0.06 [-0.21, 0.33]	
	ICGC	-0.026524047	0.688	-0.16 [-0.51, 0.19]	
	GSE14520	0.011928847	0.86	-0.20 [-0.43, 0.03]	
C3	TCGA	-0.331076183	***	-0.98 [-1.35, -0.61]	
	ICGC	-0.131423951	*	-0.93 [-1.32, -0.54]	
	GSE14520	-	-		
C5	TCGA	-0.133526804	*	-0.52 [-0.88, -0.16]	
	ICGC	-0.013502664	0.84	-0.69 [-1.09, -0.29]	
	GSE14520	0.202534108	**	-0.46 [-0.77, -0.15]	
C6	TCGA	-0.232522179	***	-1.76 [-2.37, -1.15]	
	ICGC	-0.066430692	0.314	-1.66 [-2.17, -1.14]	
	GSE14520	-0.002792824	0.967	-1.08 [-1.58, -0.58]	
C7	TCGA	-0.2302484	***	-2.17 [-2.86, -1.48]	
	ICGC	0.107486699	0.102	-1.32 [-1.85, -0.79]	
	GSE14520	-0.003304013	0.961	-1.02 [-1.48, -0.57]	

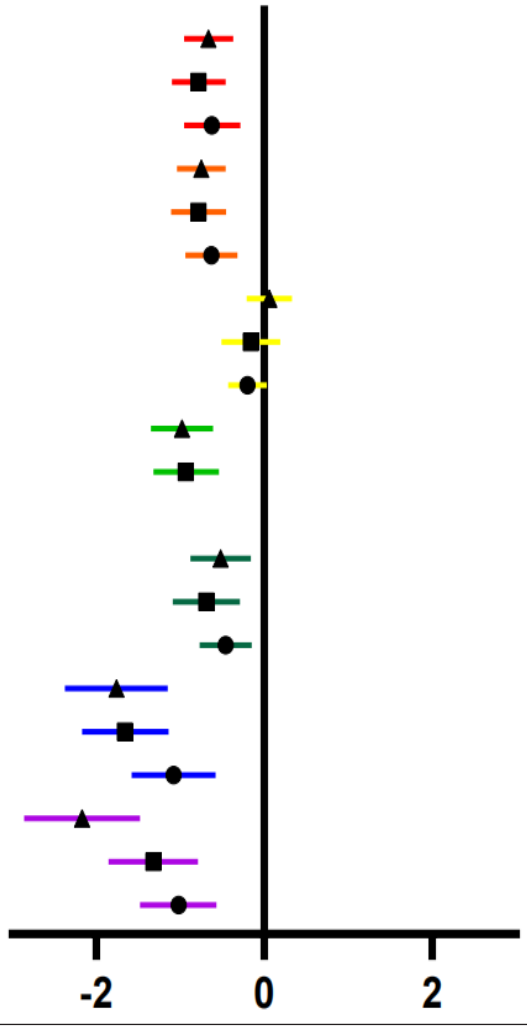

https://dx.doi.org/10.21037/tcr-21-2853